CHINESE OPTICS LETTERS

Vol. 22, No. 2 | February 2024

Real-time UWOC miniaturized system based on FPGA and LED arrays and its application in MIMO

An Huang (黄 安), Hongxi Yin (殷洪玺)*, Yanjun Liang (梁彦军), Jianying Wang (王建英), and Zhongwei Shen (沈众卫)
School of Information and Communication Engineering, Dalian University of Technology, Dalian 116024, China

*Corresponding author: hxyin@dlut.edu.cn
Received August 5, 2023 | Accepted September 20, 2023 | Posted Online February 22, 2024

In order to alleviate the impact of turbulence on the performance of underwater wireless optical communication (UWOC) in real time, and achieve high-speed real-time transmission and low cost and miniaturization of equipment, a 2×2 real-time multiple-input and multiple-output (MIMO) high-speed miniaturized UWOC system based on a field-programmable gate array (FPGA) and a high-power light-emitting diode (LED) array is designed in this Letter. In terms of multiplexing gain, the imaging MIMO spatial multiplexing and high-order modulation for the first time are combined and the real-time high-speed transmission of PAM-4 signal based on the LED array light source in 12 m underwater channel at 100 Mbps rate is implemented, which effectively improves the throughput of the UWOC system with a high-power commercial LED light source. In light of diversity gain, the system employs the diversity of repeated coding scheme to receive two identical non-return-to-zero on-off keying (NRZ-OOK) signals, which can compensate the fading or flickering sublinks in real time under the bubble-like simulated turbulence condition, and has high robustness. To our knowledge, this is the first instance of a high rate and long-distance implementation of a turbulence-resistant real-time MIMO miniaturized UWOC system based on FPGA and high-power LED arrays. With spatial diversity or spatial multiplexing capabilities, its low cost, integrity, and high robustness provide the system with important practical prospects.

Keywords: underwater wireless optical communication; MIMO; spatial diversity; spatial multiplexing.
DOI: 10.3788/COL202422.020601

1. Introduction

With the increasing demand for marine ecological monitoring and conservation, as well as resource exploration and development, there is an increasing need for higher-quality underwater communication technology. This poses a challenge in terms of ensuring the reliable and efficient communication in underwater environments. The underwater wireless optical communication (UWOC), with its advantages of high speed, low latency, and high confidentiality, can be employed to compose high-speed and real-time local area networks for short to medium ranges, or complement the underwater acoustic communication to build a hybrid network[1–5]. Compared with the UWOC system based on the laser diode (LD), the UWOC system depending on the light-emitting diode (LED) can greatly reduce the requirements of the transceiver alignment for the non-fixed position and orientation in the dynamic seawater environment. At the same time, the LED arrays can be exploited to enhance the optical signal strength to extend the transmission distance, and the high-order modulation can be utilized to improve its bandwidth utilization[6–10].

In addition, the fluctuations in the seawater temperature and salinity gradients, or the uneven distribution of bubbles, can induce ocean turbulence, which leads to the temporal and spatial variations in the refractive index of seawater. As a consequence, this turbulence can cause beam expansion, beam drift, spot jitter, and intense flickering, resulting in the signal fading during the transmission of light, which negatively impact the performance of UWOC[11,12]. The multiple-input and multiple-output (MIMO) technology has the capability to mitigate signal fading and achieve a larger field of view (FOV) through diversity reception, thereby reducing the alignment requirements between optical communication transmitters and receivers[13–15]. It can also been employed to transmit multiple signals through spatial division multiplexing, which effectively increases the communication transmission rate. However, some existing MIMO-UWOC systems have been implemented through theoretical modeling and simulation[13,15–17], and other experimental systems utilize arbitrary waveform generators (AWGs) as the signal source at the transmitter end and high-speed sampling oscilloscopes (HS-SOs) at the receiver end, and offline demodulation and data recovery using a personal computer (PC)+MATLAB. These implementations are actually semi-physical simulations with idealized processing of receiving signals rather than real-time and deployable MIMO-UWOC

Table 1. Typical MIMO-UWOC Systems and Their Parameters.

Light Source/ Photodetector	Modulation Mode	Data Rate/Link Length	MIMO Schemes	Methods	Ref., Year
LED/APD	OOK	/30 m	1 × 5 SIMO	Theoretical	[16], 2015
LED/SiPM	OOK	3 Mbps/60 m	M × 8 MIMO	Theoretical	[17], 2017
LED/PD	OOK	/3.66 m	7 × 7 MIMO	AWG/HS-SO	[18], 2012
LED/PIN	QAM	1.8 Gbps/1.2 m	1 × 4 SIMO	AWG/HS-SO	[19], 2019
LD/MPPC	NRZ-OOK	16 Mbps/50 m	1 × 2 SIMO	AWG/HS-SO	[20], 2020
LED/SiPM	NRZ-OOK	1 Mbps/10 m	6 × 3 MIMO	AWG/HS-SO	[11], 2022
LD/PMT	OOK	50 Mbps/233 m	2 × 2 MIMO	AWG/HS-SO	[21], 2022
LED/APD	NRZ-OOK, PAM-4	80 Mbps/12 m, 100 Mbps/12 m	2 × 2 MIMO	FPGA (real time)	This work

systems. Additionally, these systems are bulky, heavy, and expensive[18–21].

Therefore, this Letter designs and implements a real-time 2 × 2 MIMO miniaturized UWOC system based on field-programmable gate arrays (FPGAs) and LED arrays. Both the transmitter and receiver utilize the FPGAs for the real-time signal generation and the postprocessing, respectively. At the receiver end, the FPGA is employed for signal merging, real-time synchronization, demodulation, and decoding. Table 1 presents a comparison between several typical MIMO-UWOC system experiments and the work described in this Letter. In terms of spatial multiplexing, the real-time and high-speed transmission of 4-level pulse amplitude modulation (PAM-4) signals in the 12-m underwater channel with a rate of 100 Mbps is successfully achieved for the first time (we believe) by combining imaging MIMO spatial multiplexing with high-order modulation, and the bit error rate (BER) of the system is maintained below 2.736×10^{-3}. In comparison with existing UWOC systems based on high-power LED light sources, the insufficient original modulation bandwidth of single-input and single-output (SISO) single-channel light source is overcome, and reliable high-speed communication is implemented. In terms of spatial diversity, the experiment successfully verifies that the MIMO-UWOC system can effectively overcome the signal fading phenomenon under the turbulence conditions of different scintillation indices in 12-m underwater channels. Compared with the existing offline demodulated semiphysical simulation of the MIMO-UWOC system, the FPGA-based real-time MIMO-UWOC diversity merging receiver system can realize real-time compensation for fading links so as to alleviate the impact of underwater turbulence on communication performance. To our knowledge, this is the first reported high-rate, long-distance implementation of a turbulence-resistant real-time MIMO miniaturized UWOC system based on FPGA and high-power LED arrays, with the option to utilize diversity gain or multiplexing gain, and its low cost, integrity, and high robustness make the system of great practical value.

2. Method

Since the refractive index of light in seawater is influenced by physical factors like bubbles, temperature gradient, salinity gradient, etc., it generates random fluctuations, which severely impacts the UWOC in practical applications. The underwater optical turbulence (UOT) leads to fluctuation (blinking) of the received optical signal, even resulting in communication link interruptions. In this study, we propose a 2 × 2 spatial diversity system to mitigate turbulence effects by providing multiple independent fading copies of information symbols for the receiver. This approach reduces the probability of deep fading of signals and enhances system performance. The optical turbulence gives rise to the random fluctuation of the received light intensity, which can be quantitatively described by the probability distribution function (PDF) and the scintillation index. In the practical application of UWOC, the specific aperture size of the optical lens at the front end of the detector is much larger than the transverse coherence length of the light, and the aperture average effect will significantly reduce the fluctuation of the received light signal[22]. A large number of field experiments show that considering the aperture averaging effect, the PDF of the received light intensity under the underwater weak turbulence can be well represented by a lognormal distribution function[23], i.e.,

$$f(I) = \frac{1}{I\sigma\sqrt{2\pi}} \exp\left(-\frac{(\ln(I/I_0) - \mu)^2}{2\sigma^2}\right), \tag{1}$$

where I_0 represents the average received light intensity, μ is the average logarithmic light intensity; σ^2 is the scintillation index, which is an important index to measure flicker and fading caused by turbulence, and is defined as[13]

$$\sigma^2(r, L, \lambda) = \frac{E(I^2(r, L, \lambda)) - E^2(I(r, L, \lambda))}{E^2(I(r, L, \lambda))}, \tag{2}$$

where $I(r, L, \lambda)$ is the instantaneous light intensity received at the position vector of (r, L) under the condition of optical wavelength of λ, r is the position coordinate (x, y), L is the length of the communication link, and $E(\cdot)$ represents the mathematical expectation.

In the experiment, a 15-W air pump is utilized to simulate the bubble turbulence generation. A hose is inserted into a 12-m water pipe to evaluate the spatial diversity reception performance of the MIMO-UWOC system under three distinct scintillation indices. In the absence of bubbles, the MIMO-UWOC system receives an optical power of 323.78 μW after transmitting through a 12-m clear underwater channel. After the pump is turned on, three levels of bubbles are generated to simulate turbulences with different scintillation indices, and the received light power is greatly attenuated due to the absorption, scattering, and turbulence of bubbles. The statistical diagram obtained based on the test results is shown in Fig. 1. The figure shows the PDF histogram obtained by using the UT385 optical power meter to sample 100 groups of instantaneous optical power, which can be well represented by the lognormal distribution function. When the sampled instantaneous optical power is substituted into Eq. (2), the scintillation indices of σ^2 corresponding to three different intensity turbulences can be calculated as 0.0014, 0.0239, and 0.1538, respectively.

In traditional wireless communication, the spatial diversity is extensively applied to mitigate the channel's deep fading. To achieve optimal performance, the subchannels of the MIMO system's diversity receptions should be independent from one another, which implies that the receiver spacing must exceed the transverse coherence length of ρ_0. By leveraging the conventional free-space optics theory of atmospheric optical turbulence and the UOT spectral model, the value of ρ_0 in the MIMO-UWOC system can be determined as[22]

$$\rho_0 = \left(44.2K_3\left(\frac{2\pi}{\lambda}\right)^2 L\right)^{-\frac{3}{5}}, \tag{3}$$

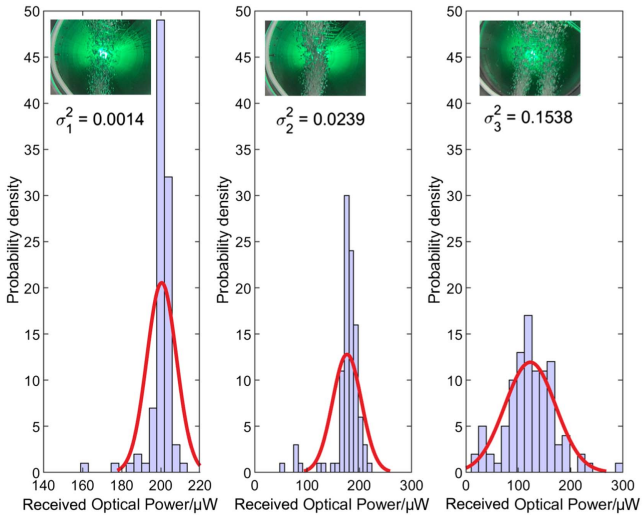

Fig. 1. PDF histograms and scintillation index under the presence of air bubbles.

where λ is the wavelength of the beam, L is the length of the communication link, $K_3 = \chi\varepsilon^{-1/3}$ is the constant that determines the turbulence intensity, ε is the kinetic energy dissipation rate, and χ is the intensity of the temperature gradient. We can see that ρ_0 gradually decreases with the increases in propagation length and the turbulence intensity. In medium to strong turbulences, when the propagation length is greater than 12 m, ρ_0 is much less than 1 cm. To enhance the average aperture effect and meet diversity requirements, the size of each receiving optical lens is set to 100 mm, and the center distance between adjacent lenses is $d = 20$ cm.

For the optical transmitter part of the 2×2 MIMO-UWOC system, in order to improve the transmission distance, two green 45×1 W high-power LED array light sources with 517 nm wavelength are employed, and a convex lens module with a 30° divergence angle is equipped. The light source chip adopts a 3030 encapsulation SMT LED chip whose original bandwidth is measured up to 22.6 MHz. To achieve the high-speed data transmission with the LED array light source, a frequency domain pre-equalization circuit is utilized at the transmitter to improve the frequency response characteristics of the commercial LED[24,25].

At the optical receiving end of MIMO-UWOC, we adopt a dual-channel avalanche photodiode-automatic gain control amplifier (APD-AGC) structure, where the AGC sets its gain coefficient for the gain combination. Subsequently, the converted analog signals are input to two AD9233 (analog-to-digital converter, ADC) modules with a 125 MSa/s sampling rate, and finally the diversity combination reception and real-time synchronous demodulation of the two signals are realized by the FPGA. The APD-AGC optical receiver can effectively deal with the flicker or fluctuation of light intensity caused by complex factors such as the change of the axial declination angle of the optical link, the variation of transmission distance, and jitter and turbulence; moreover, it has high robustness. In the part of bit error detection at the receiving end, a bit error detection module is designed in the FPGA of the optical receiver to perform real-time bit error statistics by connecting to the received bit stream. The SignalTap logic analyzer can be exploited through the USB high-speed serial port to view the BER and signal status in real time and collect the received raw data at the PC end for bit error verification.

3. Result and Discussion

In terms of spatial diversity, this Letter adopts the most common MIMO diversity scheme, in which all transmitters send the same signal, i.e., the repetitive coding (RC); its system block diagram is shown in Fig. 2. In the diversity receiving process of the MIMO system receiver, when one signal deteriorates or is interrupted briefly due to the absorption, scattering, and turbulence link of bubbles, the other signal passes through to ensure the integrity of communication. This 2×2 MIMO-UWOC system can be represented by the following discrete time model as

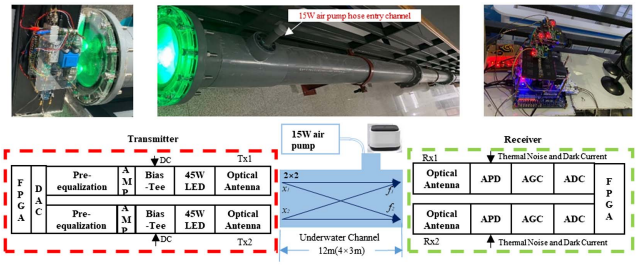

Fig. 2. Block diagram of a miniaturized real-time MIMO-UWOC diversity gain system based on FPGA.

$$\begin{bmatrix} f_1 \\ f_2 \end{bmatrix} = \begin{bmatrix} h_{11} & h_{12} \\ h_{21} & h_{22} \end{bmatrix} \begin{bmatrix} x_1 \\ x_2 \end{bmatrix} + \begin{bmatrix} n_1 \\ n_2 \end{bmatrix}. \tag{4}$$

It can also be simply expressed as $f = \boldsymbol{Hx} + \boldsymbol{n}$, where $\boldsymbol{x}$ is the transmitted signal, $\boldsymbol{n}$ indicates the channel noise vector, and $\boldsymbol{H}$ denotes the channel gain matrix, where h_{ij} represents the channel gain from the jth sending antenna to the ith receiving antenna. The system diversity combining adopts the equal gain combining (EGC) scheme, which can be expressed as

$$Z_{\mathrm{Div}} = c_1 f_1 + c_2 f_2 + N = \sum_{l=1}^{2} c_l f_l + N. \tag{5}$$

In the formula, f and c represent the signals received by the L-channels and their weights, respectively, and Z_{Div} is the signals after the diversity merging. By adjusting the AGC, the original specific weights are $c_1 = c_2 = 0.5$. Suppose that the received optical power of f_1 channel signal is sharply attenuated by the deep fading and even exceeds the recovery capability of the AGC; at this time, the weight c_1 of the affected signal is greatly reduced, and the weight c_2 of the less affected signal is relatively increased. The diversity-received two non-return-to-zero on-off keying (NRZ-OOK) signals can still recover its original correct digital signal through the zero-crossing decision (ZCD) and the interpolation bit synchronization after the merging processing of Eq. (5) is performed by the FPGA.

The SignalTap logic analyzer checks the results of real-time reception of f_1 and f_2 signals and the results of merging, ZCD and bit synchronization (BSY), as shown in Fig. 3. The BER performance of the NRZ-OOK pulse-shaping signal of

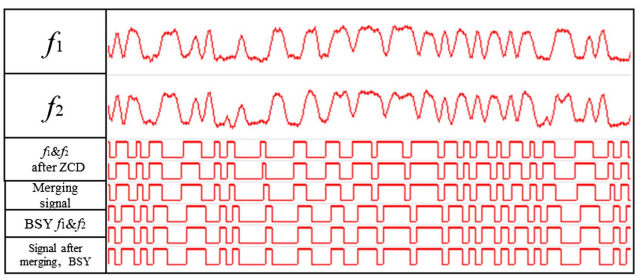

Fig. 3. Results of real-time reception of f_1 and f_2 signals, diversity reception and merging, ZCD, and bit synchronization from SignalTap logic analyzer.

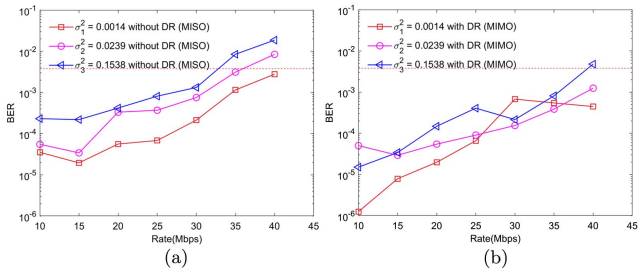

Fig. 4. (a) BER curves of MISO in three types of scintillation intensity turbulences; (b) BER curves of MIMO diversity reception in three scintillation intensity turbulences.

the MISO-UWOC (multiple-input and single-output) system scheme and the real-time diversity-receiving scheme of the MIMO-UWOC system under three scintillation indices is verified through our experiments, as shown in Figs. 4(a) and 4(b), both of which use the FPGA to realize real-time synchronous transmission. It can be observed that, in the diversity scheme with the same transmission rate, as the flicker index increases, the system performance deteriorates due to the impact of flickering and fading. By using multiple independent antennas for data transmission and reception, even if certain transmission paths experience interference or fading, other transmission paths can still provide reliable transmission. Compared with the 2×2 MIMO-UWOC system, the 2×1 MISO-UWOC system has only one optical antenna for data reception, which cannot take full advantage of multipath transmission. Comparing the BER curves of MIMO and MISO in Fig. 5, it is evident that the overall BER of the MIMO diversity merging reception scheme is significantly lower than that of the MISO scheme without diversity-merging reception. The bit error performance of the MIMO scheme remains within the forward error correction (FEC) threshold of 3.8×10^{-3} for flicker index values less than 0.1538 and transmission rates below 40 Mbps. In summary, the MIMO diversity has better resistance to interference and reliability. The system can overcome the impact of bubble-induced turbulence in real time and effectively improve system performance.

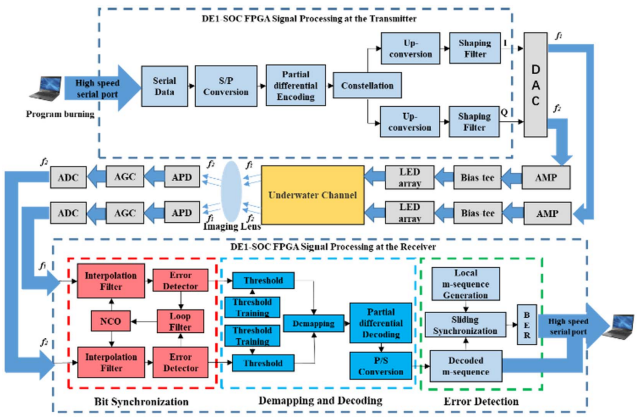

Fig. 5. Imaging PAM-4-MIMO-UWOC system based on FPGA.

In terms of spatial multiplexing, the MIMO-UWOC system described in this Letter employs optical lenses to map the transmitted signal to the corresponding detector through the imaging mode, namely, the imaging MIMO. As shown in Fig. 5, the optical imaging method, which has low hardware complexity, is employed to demultiplex to recover two relatively independent original signals. The system improves the frequency spectrum utilization and the throughput of the system by means of the spatial multiplexing, which can solve the problem of original low bandwidth of commercial high-power LED array light sources under SISO scheme. Previous studies have shown that the imaging MIMO-UWOC has lower spatial correlation than the non-imaging MIMO-UWOC, so that it can achieve higher multiplexing gain[26].

The dual-channel NRZ-OOK pulse-shaping signals and the PAM-4 signals are utilized in the MIMO spatial multiplexing demonstration, and their performances are compared with that of the SISO-UWOC real-time communication system, respectively.

For the SISO-UWOC system, by combining the hardware frequency domain pre-equalization circuit, it can realize real-time synchronous transmission of an NRZ-OOK pulse-shape signal at 40 Mbps rate, and the BER at 40 Mbps is 9.154×10^{-4}, which is lower than the threshold of FEC. However, in the imaging MIMO-UWOC system proposed in this Letter, when two different NRZ-OOK pulse-shaping signals are transmitted in real time using two parallel m-pseudo-random sequences, with lengths of $2^8 - 1$ and $2^{15} - 1$, respectively, via spatial multiplexing, the total transmission rate for both channels is maintained at 80 Mbps. The BER consistently remains below 1.361×10^{-3}, which is also below the FEC threshold, as depicted in Fig. 6(a). In summary, it is evident that the imaging MIMO multiplexing mode significantly enhances the throughput of the UWOC system, albeit with a slight decrease in the signal-to-noise ratio (SNR) of the sublinks.

Subsequently, the high-order modulation and the MIMO multiplexing gain are combined for the first time to transmit dual PAM-4 signals to further improve spectrum utilization, as shown in Fig. 5. The PAM-4 is a modulation technology that utilizes four different signal levels for signal transmission. As a popular signal transmission technology for the next-generation high-speed interconnects, the PAM-4 signals feature an additional two signal levels compared to traditional NRZ-OOK signals. NRZ-OOK signals use high- and low-signal levels to represent digital logic signals of 1 and 0, respectively, allowing for the transmission of 1 bit of logical information per cycle. On the other hand, the PAM-4 signals employ four different signal levels, namely, 00, 01, 10, and 11, enabling the transmission of 2 bits of logical information per symbol cycle. Therefore, within the same symbol period, the bit rate of PAM-4 signals is twice that of NRZ-OOK signals. The signal source utilizes an m-sequence of length $2^{15} - 1$, which is transformed through serial/parallel conversion into a parallel sequence with 4 bits per symbol. After PAM-4 encoding mapping on the preceding and succeeding 2 bits of each symbol, a dual baseband signal

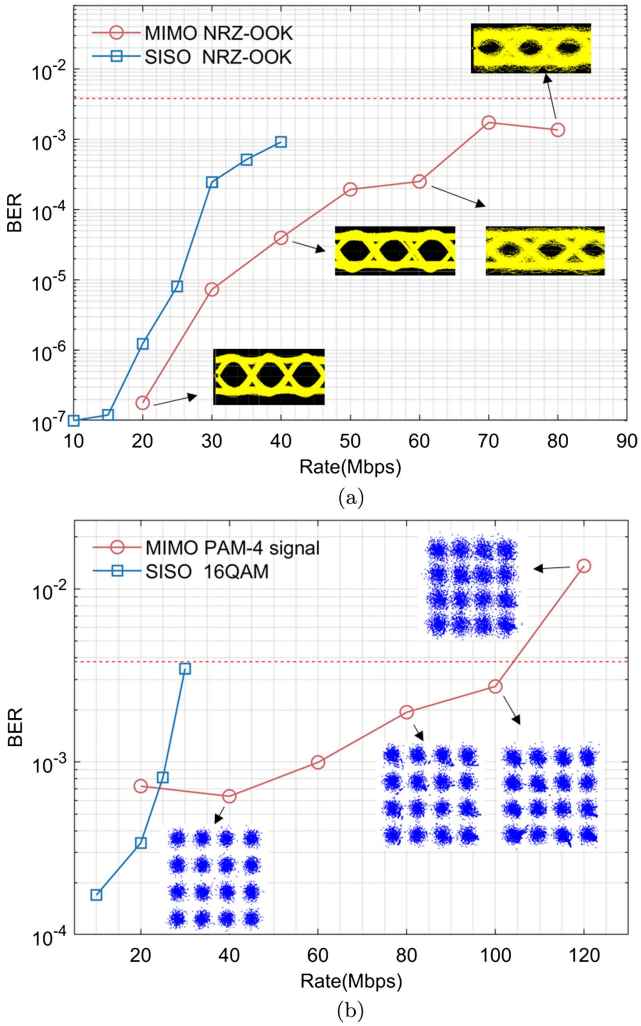

Fig. 6. Imaging MIMO-UWOC system spatial multiplexing BER curve for (a) NRZ-OOK signal BER; (b) PAM-4 signal.

is generated with four distinct voltage levels. Then two PAM-4 signals are modulated to the optical carrier. The signal of optical receiving end is demultiplexed through the lens imaging to recover two channels of PAM-4 signals, and then, the pseudo-random sequence code stream is restored through the interpolation bit synchronization and two independent decision threshold trainings, the constellation inverse mapping, and parallel/serial conversion, whose BER and corresponding constellation diagram are shown in Fig. 6(b). The imaging MIMO-UWOC system can significantly improve the transmission rate under the condition of limited bandwidth of commercial high-power LED arrays in combination with high-order modulation, and the BER is less than 2.736×10^{-3} at a transmission rate of 100 Mbps. In our previous work[10], we adopted the same high-power LED arrays and adopted a 16QAM-SISO-UWOC scheme to achieve effective real-time communication in 12 m underwater channels, only at a rate of 30 Mbps within the FEC threshold, which is worse than the performance of the PAM-MIMO-UWOC system proposed in this Letter, as shown

in Fig. 6(b). The MIMO spatial division multiplexing is used to transmit the PAM-4 signals, which effectively avoids the constellation rotation caused by the carrier synchronization in the *m*-QAM-SISO-UWOC (*m*-ary quadrature amplitude modulation), effectively solves the problem of difficult synchronization in the UWOC system with high-order modulation, and thus greatly improves system performance. Its cost is that as the rate increases, the horizontal offsets between the transmitting and receiving optical paths will affect communication performance. From the perspective of MIMO multiplexing applications of NRZ-OOK and PAM-4 signals, the multiplexing system can meet the needs of reliable and efficient communication in different underwater scenarios.

4. Conclusion

In this Letter, an FPGA-based anti-turbulence real-time 2×2 MIMO integrated miniaturized UWOC system is proposed and implemented for the first time, we believe. In terms of spatial diversity gain, the turbulences with three different scintillation indices are generated by the air pump bubble simulation. Then, the FPGA-based MIMO-UWOC system successfully achieves the real-time diversity-merging reception in the 12-m underwater turbulent channel, which compensates for fading and flickering sublinks in real time, greatly improving system performance. In terms of spatial multiplexing gain, the imaging MIMO-UWOC system is designed, combined with a T-bridge pre-equalization circuit, which effectively improves the throughput of the UWOC system based on commercial LED light sources. The NRZ-OOK signal with 80 Mbps rate and the PAM-4 signal with 100 Mbps rate are transmitted under the 12-m underwater channel within the FEC decision threshold of 3.8×10^{-3}, which can solve the problem of insufficient modulation bandwidth of high-power commercial LED arrays under the traditional SISO scheme. Compared with previous studies in the literature, the designed system is in a leading position in performance and fills the gap in the experiment of miniaturized real-time MIMO-UWOC systems based on the FPGA, which will play an important role in the high-speed network detection of underwater robot clusters in the future.

Acknowledgements

This work was supported by the National Natural Science Foundation of China (NSFC) (No. 61871418).

References

1. M. F. Ali, D. N. K. Jayakody, Y. Chursin, *et al.*, "Recent advances and future directions on underwater wireless communications," Arch. Comput. Method **27**, 1379 (2020).
2. C. Fei, X. Hong, G. Zhang, *et al.*, "16.6 Gbps data rate for underwater wireless optical transmission with single laser diode achieved with discrete multi-tone and post nonlinear equalization," Opt. Express **26**, 34060 (2018).
3. C. Fang, S. Li, Y. Wang, *et al.*, "High-speed underwater optical wireless communication with advanced signal processing methods survey," Photonics **10**, 811 (2023).
4. M. Salim, O. Nameer, S. Adnan, *et al.*, "Underwater optical wireless communication system performance improvement using convolutional neural networks," AIP Adv. **13**, 045302 (2023).
5. H. Yang, Q. Yan, M. Wang, *et al.*, "Synchronous clock recovery of photon-counting underwater optical wireless communication based on deep learning," Photonics **9**, 884 (2022).
6. X. Yang, Z. Tong, H. Zhang, *et al.*, "7-M/130-Mbps LED-to-LED underwater wireless optical communication based on arrays of series-connected LEDs and a coaxial lens group," J. Lightwave Technol. **40**, 5901 (2022).
7. P. Wang, C. Li, and Z. Xu, "A cost-efficient real-time 25 Mb/s system for LED-UOWC: design, channel coding, FPGA implementation, and characterization," J. Lightwave Technol. **36**, 2627 (2018).
8. H. J. Son, J. I. Kang, T. Q. M. Nhat, *et al.*, "Study on underwater optical communication system for video transmission," J. Ocean Eng. Sci. **32**, 143 (2018).
9. B. Dong, S. Tong, P. Zhang, *et al.*, "Design of a 20 m underwater wireless optical communication system based on blue LED," Chin. Opt. **14**, 1451 (2021).
10. A. Huang, H. Yin, X. Ji, *et al.*, "Research and implementation of miniaturized UWOC system based on field programmable gate array and high-power LED array light source," Acta Opt. Sin. **44**, 0606002 (2024).
11. J. Li, D. Ye, K. Fu, *et al.*, "Single-photon detection for MIMO underwater wireless optical communication enabled by arrayed LEDs and SiPMs," Opt. Express **29**, 25922 (2021).
12. H. Wen, H. Yin, X. Ji, *et al.*, "Modeling and performance analysis of underwater wireless optical absorption, scattering, and turbulence channels employing Monte Carlo-multiple phase screens," Appl. Opt. **62**, 6883 (2023).
13. M. V. Jamali, M. J. A. Salehi, and F. Akhoundi, "Performance studies of underwater wireless optical communication systems with spatial diversity: MIMO scheme," IEEE Trans. Wirel. Commun. **65**, 1176 (2017).
14. Y. B. Bedir and E. E. Elsayed, "Performance enhancement of an orbital-angular-momentum-multiplexed free-space optical link under atmospheric turbulence effects using spatial-mode multiplexing and hybrid diversity based on adaptive MIMO equalization," IEEE Access **7**, 84401 (2019).
15. J. Wang, H. Yin, X. Ji, *et al.*, "Performance analysis of MIMO-mQAM system with pointing errors and beam spreading in underwater málaga turbulence channel," J. Mar. Sci. Eng. **11**, 633 (2023).
16. W. Liu, Z. Xu, and L. Yang, "SIMO detection schemes for underwater optical wireless communication under turbulence," Photonics Res. **3**, 48 (2015).
17. P. Leon, F. Roland, L. Brignone, *et al.*, "A new underwater optical modem based on highly sensitive silicon photomultipliers," in *OCEANS-Aberdeen* (2017), p. 1.
18. J. A. Simpson, B. L. Hughes, and J. F. Muth, "Smart transmitters and receivers for underwater free-space optical communication," IEEE J. Sel. Area Commun. **30**, 964 (2012).
19. J. Li, F. Wang, M. Zhao, *et al.*, "Large-coverage underwater visible light communication system based on blue LED employing equal gain combining with integrated PIN array reception," Appl. Opt. **58**, 383 (2019).
20. M. Zhao, X. Li, X. Chen, *et al.*, "Long-reach underwater wireless optical communication with relaxed link alignment enabled by optical combination and arrayed sensitive receivers," Opt. Express **28**, 34450 (2020).
21. X. Chen, Y. Dai, Z. Tong, *et al.*, "Demonstration of a 2×2 MIMO-UWOC system with large spot against air bubbles," Appl. Opt. **61**, 41 (2022).
22. L. C. Andrews, R. L. Philips, and C. Y. Hopen, *Laser Beam Scintillation with Applications* (SPIE, 2001).
23. F. S. Vetelino, C. Young, L. Andrew, *et al.*, "Aperture averaging effects on the probability density of irradiance fluctuations in moderate-to-strong turbulence," Appl. Opt. **46**, 2099 (2007).
24. A. Liu, R. Zhang, B. Lin, *et al.*, "Multi-degree-of-freedom for underwater optical wireless communication with improved transmission performance," J. Mar. Sci. Eng. **11**, 48 (2023).
25. X. Huang, Z. Wang, J. Shi, *et al.*, "1.6 Gbit/s phosphorescent white LED based VLC transmission using a cascaded pre-equalization circuit and a differential outputs PIN receiver," Opt. Express **23**, 22034 (2015).
26. C. B. Naila, T. Nakamura, H. Okada, *et al.*, "Evaluation of conventional and imaging MIMO OWC systems using linear array design," IEEE Photonics J. **14**, 7350709 (2022).